

Influence of Temperature and Carbonation on Chloride Induced Corrosion of Carbon Steel in Concrete Pore Solutions

Jie Zha, Linhua Jiang*, Peng Xu, Ming Jin, Peng Jiang

College of Mechanics and Materials, Hohai University, Nanjing 210098, PR China.

*E-mail: lhjiang@hhu.edu.cn

Received: 5 October 2021 / Accepted: 8 November 2021 / Published: 6 December 2021

The effects of the temperature, carbonation, and different types of synthetic solutions on chloride corrosion of steel reinforcement were investigated in this paper. A relatively wide range of temperatures (from 5°C to 60°C) and three synthetic solutions (Ca(OH)₂ + KOH + NaOH solution, the cement and cement-slag extracts) were applied. In addition, a high concentration of bicarbonate ions (0.2 mol/L) was used to simulate the effect of carbonation. The open-circuit potential and corrosion current density were obtained from the linear polarization resistance and EIS results to evaluate the corrosion resistance of samples. Higher temperatures increase the corrosion of steel above 20°C. This is accounted for by the acceleration of both the corrosion reaction and dissolution of passive films. The lower temperature (5°C) similarly promotes corrosion due to the increased dissolved oxygen in the solutions. The existence of HCO₃⁻ inhibits the corrosion process in traditional synthetic solutions under 40°C but promotes corrosion at 60°C, which can be attributed to the buffering influence of ions and decomposition. The traditional synthetic solutions and cement extracts are more appropriate for simulation of the effect of temperature and carbonation.

Keywords: temperature, carbonation, chloride ions, reinforcement corrosion, cement, slag

1. INTRODUCTION

Corrosion of reinforcing steel is one of the main durability problems in construction. This will mainly cause the deterioration of reinforced concrete structures, especially in aggressive environments. Due to the corrosion of steel reinforcement, the service-life of structures can be remarkably reduced. This will not only bring the security risks in structures but also cause major economic losses.

Chloride ion is one of the most common ions in steel corrosion. It can be introduced into concrete structures by the deicing salts, the water or soil around them, etc. The ions then will gradually penetrate through the concrete cover to the surface of the steel. When concentrations of Cl⁻ accumulate to a certain

value, passive layers of the steel will be destroyed. A certain concentration value is regarded as the critical chloride level (CTL)[1]. Many investigations have been conducted on the corrosion behaviors and mechanics of steel with chloride ions. It has been found that many factors are related to chloride corrosion results, such as sulfate ions[2], chloride salt types, and the pH values of concrete pore solutions[3].

Among all the factors, temperature and carbon dioxide (CO₂) are worth attention. Different corrosion regions correspond to varying corrosion temperatures. For example, corrosion often occurs at low temperatures if chloride ions are introduced by deicing salts in severely cold areas. For corrosion occurring in tropical regions, the temperature is much higher[4]. Numerous works have focused on the effect of high temperatures due to the slow reaction rates at low temperatures. A higher temperature accelerates the kinetics of most chemical reactions, including electrochemical reactions during chloride corrosion. Over 10°C, the corrosion current density was reported to substantially increase with increasing temperature[5-8]. Meanwhile, low temperatures also showed acceleration effects on corrosion rates[9]. Apart from the temperature, the existence of CO₂ also affects the corrosion behavior of steel. CO₂ gas can diffuse through concrete and react with some hydration products, such as calcium hydroxide (CH). Then the pH values of the concrete pore solutions will change, as will the concrete pore structures. It has been reported that low levels of CO₃²⁻ and HCO₃⁻ in pore solutions accelerate chloride corrosion, but high levels do the opposite[10]. The effect of CO₂ could be more obvious in concrete with slags due to the smaller amount of CH. Furthermore, methods for simulating concrete pore solutions are also worth considering. Two main methods are usually adopted: synthetic solutions aiming to reproduce the composition and the aqueous phase extracted from cement pastes. The synthetic pore solutions may not fully represent the actual pore solutions in concrete[11]. However, due to the heterogeneity in the concrete structure[12] and the small amount of water extracted from pastes[13], it is still a common option for researchers.

In this study, the effects of the temperature, carbonation, and types of synthetic solutions on chloride corrosion of reinforcement were investigated. Three kinds of synthetic solutions were chosen in the test: Ca(OH)₂ + KOH + NaOH solution, cement and cement-slag extracts. These were intended to simulate the actual pore environment in concrete, and to determine if they were appropriate considering the temperature changes. A relatively wide range of temperature variations (5°C - 60°C) was applied. A temperature of 5°C was designed to investigate the effect of low temperatures on steel corrosion. It is easily ignored because serious corrosion is usually considered to occur at high temperatures. Various electrochemical measurements were conducted to monitor the corrosion of reinforced steel under different conditions. Further analyses were based on the open-circuit potential (E_{corr}), corrosion current density (i_{corr}) and electrochemical impedance spectroscopy (EIS) results.

2. EXPERIMENTAL

2.1. Materials and specimen preparation

A simplified flow diagram of the test procedures in this paper is shown in Fig 1. Cylindrical carbon steel specimens 20 mm in diameter and 10 mm in length were used in this study. The chemical

composition of the steel is listed in Table 1. A copper wire was welded to one cross section of the steel specimen, and then the whole specimen was sealed in epoxy resin with only the other cross section exposed. This exposed surface was used for the electrochemical test and was polished with #150, #400, #800, #1000 and #1200 SiC emery paper. Finally, the specimen was cleaned with acetone, washed in distilled water, dried in air, and stored for subsequent tests. The cement used in the present work was P. II 42.5 Portland cement supplied by Anhui Conch Cement. The slag was the ground granulated blast furnace slag (GGBFS) produced by NANGKANG K.WAN. Their chemical compositions are presented in Table 2.

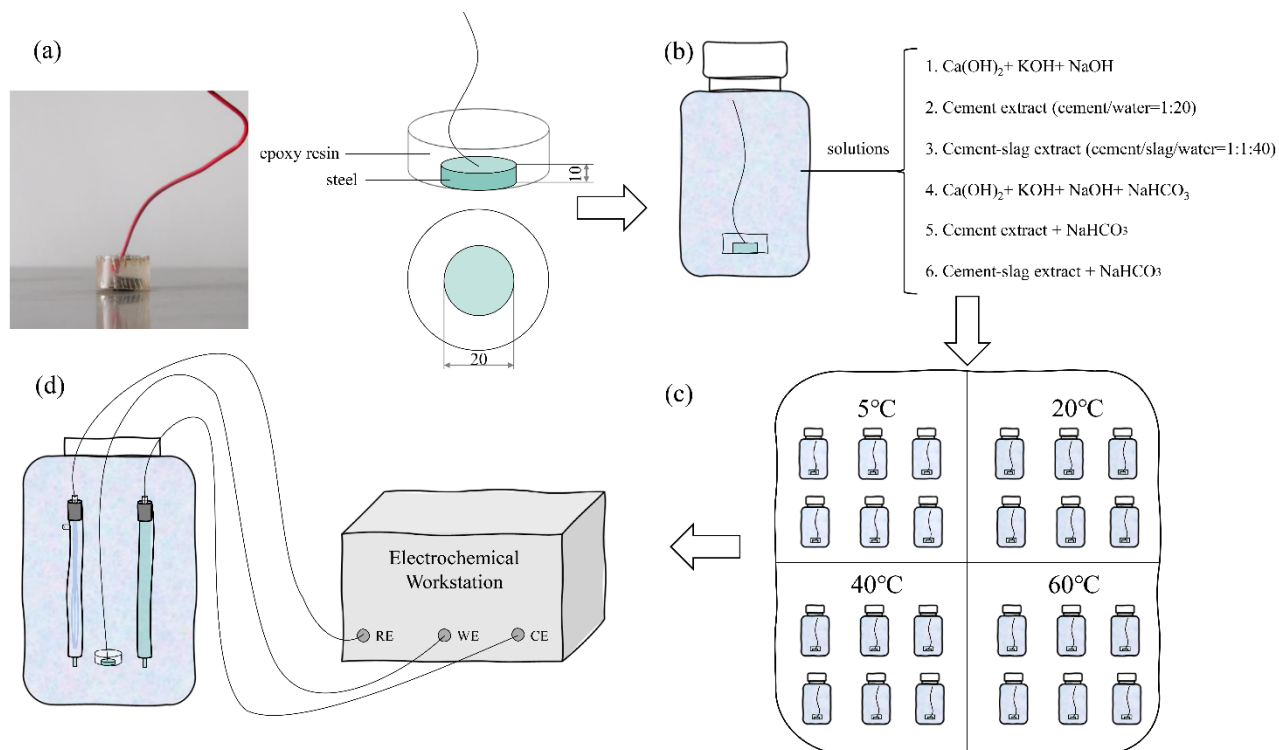


Figure 1. Flow diagram of test procedures: (a) Steel samples, (b) Solutions, (c) Curing temperatures, (d) Electrochemical tests

Table 1. Chemical composition of steel reinforcement (wt.%)

C	Si	Mn	S	P
0.22	0.30	0.65	0.05	0.045

Table 2. Chemical compositions of cement and slag (wt.%)

Material	CaO	SiO ₂	Al ₂ O ₃	Fe ₂ O ₃	MgO	SO ₃	LOI*
cement	60.4	22.6	4.9	4.3	3.2	2.8	1.2
slag	38.8	32.3	14.5	10.3	0.4	0.17	0.15

*LOI is the abbreviation for Loss on Ignition.

2.2. Exposure solutions and temperatures

Several synthetic solutions were prepared in the work reported in this paper. The first was a saturated $\text{Ca}(\text{OH})_2$ solution with KOH and NaOH added, which was originally proposed by Macias et al.[13]. The concrete pore solution was regarded as an oversaturated solution of $\text{Ca}(\text{OH})_2$ with other ions added. As a typical synthetic solution, it is still widely used[3, 14]. The two other solutions were the cement and cement-slag extracts. They were obtained by dissolving 100 g cement or slag powder in 2 L distilled water. The mixture was stored in a sealed container for 28 days, and then crushed and screened to obtain the final extract. Compared to the first synthetic solution, the extract solutions contained more ions, such as Al^{3+} and SO^{4-} . These could better resemble the actual pore environment of concrete, especially concrete with added slag [15]. Sodium bicarbonate was added to simulated the effect of carbonation on chloride-induced corrosion of steel reinforcement [3, 14]. The compositions and pH values of all solutions are listed in Table 3. Chloride ions, supplied by sodium chloride, were added at 0.01 mol/L every two days after prepassivation.

Table 3. Compositions and pH values of the simulated concrete pore solutions

Solution	Composition	pH
1	Saturated $\text{Ca}(\text{OH})_2$ +0.175 M KOH+0.1 M NaOH	12.9
2	Cement extract (cement/water=1:20)	12.7
3	Cement-slag extract (cement/slag/water=1:1:40)	12.1
4	Saturated $\text{Ca}(\text{OH})_2$ +0.175 M KOH+0.1 M NaOH+0.2 M NaHCO_3	9.5
5	Cement extract (cement/water=1:20) +0.2 M NaHCO_3	9.4
6	Cement-slag extract (cement/slag/water=1:1:40) +0.2 M NaHCO_3	9.2

Four temperatures were chosen in the study to evaluate the effect of temperature on chloride-induced reinforcement corrosion: 5, 20, 40 and 60°C. They were designed to simulate the winter construction temperature, the standard curing temperature, the outdoor temperature in summer and the surface temperature of construction in direct sunlight in summer.

2.3. Electrochemical measurement and morphology observation

The classical 3-electrode system was employed during the electrochemical experiments with the PARSTAT 2273 electrochemical workstation. The steel specimen was used as the working electrode. A saturated calomel electrode and a platinum electrode served as the reference electrode and the counter electrode, respectively.

Before the tests, all steel specimens were immersed in saturated $\text{Ca}(\text{OH})_2$ solution for 7 days for prepassivation[16]. Their surface conditions were deemed to be the same. Then they were placed in the corresponding experimental solutions at the experimental temperatures. EIS and linear polarization resistance tests were carried out every two days at 20°C. To achieve the testing temperature (20°C), samples corroded at other temperatures (5, 40 and 60°C) were moved to the testing room in advance. The EIS measurements were conducted in a frequency range from 100 kHz to 10 mHz. Linear

polarization resistance tests were performed in the potential range from -10 mV to +10 mV with a scan rate of 0.166 mV/s. The data analysis was conducted using ZSimpWin software with a proper electrical equivalent circuit. After the electrochemical test, the morphology of each steel sample was observed using scanning electron microscope (SEM, JSM-6360LV SEM instrument).

3. RESULTS AND DISCUSSION

3.1. Morphology of steel

The morphology of steel samples immersed in different solutions is shown in Fig. 2. Severe damage could be found on the surface of steel in solutions with chloride ions. In contrast, the steel in saturated $\text{Ca}(\text{OH})_2$ solutions had a smooth surface without any corrosion pits.

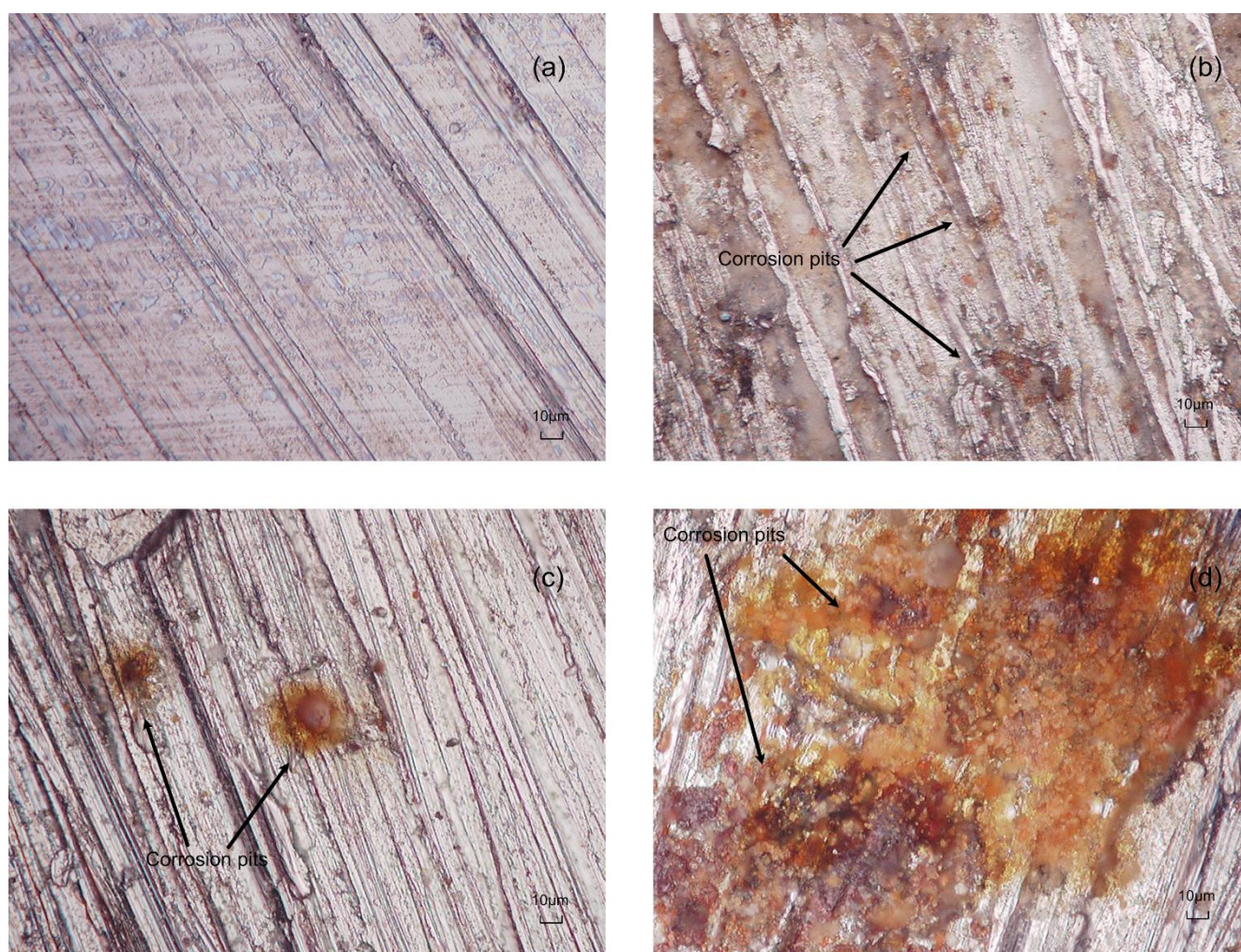


Figure 2. SEM images of samples immersed in: (a) saturated $\text{Ca}(\text{OH})_2$ before the test, (b) Solution 2 with 0.09 mol/L Cl^- at 20°C, (c) Solution 5 with 0.09 mol/L Cl^- at 20°C, and (d) Solution 2 with 0.09 mol/L Cl^- at 60°C

Temperatures and bicarbonate ions both had effects on the corrosion behavior of steel samples. More serious damage can be seen on the surface of the samples at 60°C in Fig. 2.(d). It was covered with a large quantity of corrosion products. In contrast, there were only a few corrosion pits at 20°C. In addition, with bicarbonate ions in the solutions, the number of corrosion pits comparatively decreased. The corrosion was suppressed to some extent.

3.2. Corrosion potential

The developments of E_{corr} for samples in solutions are shown in Fig. 3. Without chloride ions, the E_{corr} values for all samples were over -200 mV. With the increasing concentration of chloride ions, there was a consistent downward trend in E_{corr} for all samples. In addition, an abrupt drop in E_{corr} for the samples appeared at a certain level of chloride ions. This was a sign of the breakdown of passive films caused by chloride ion corrosion.

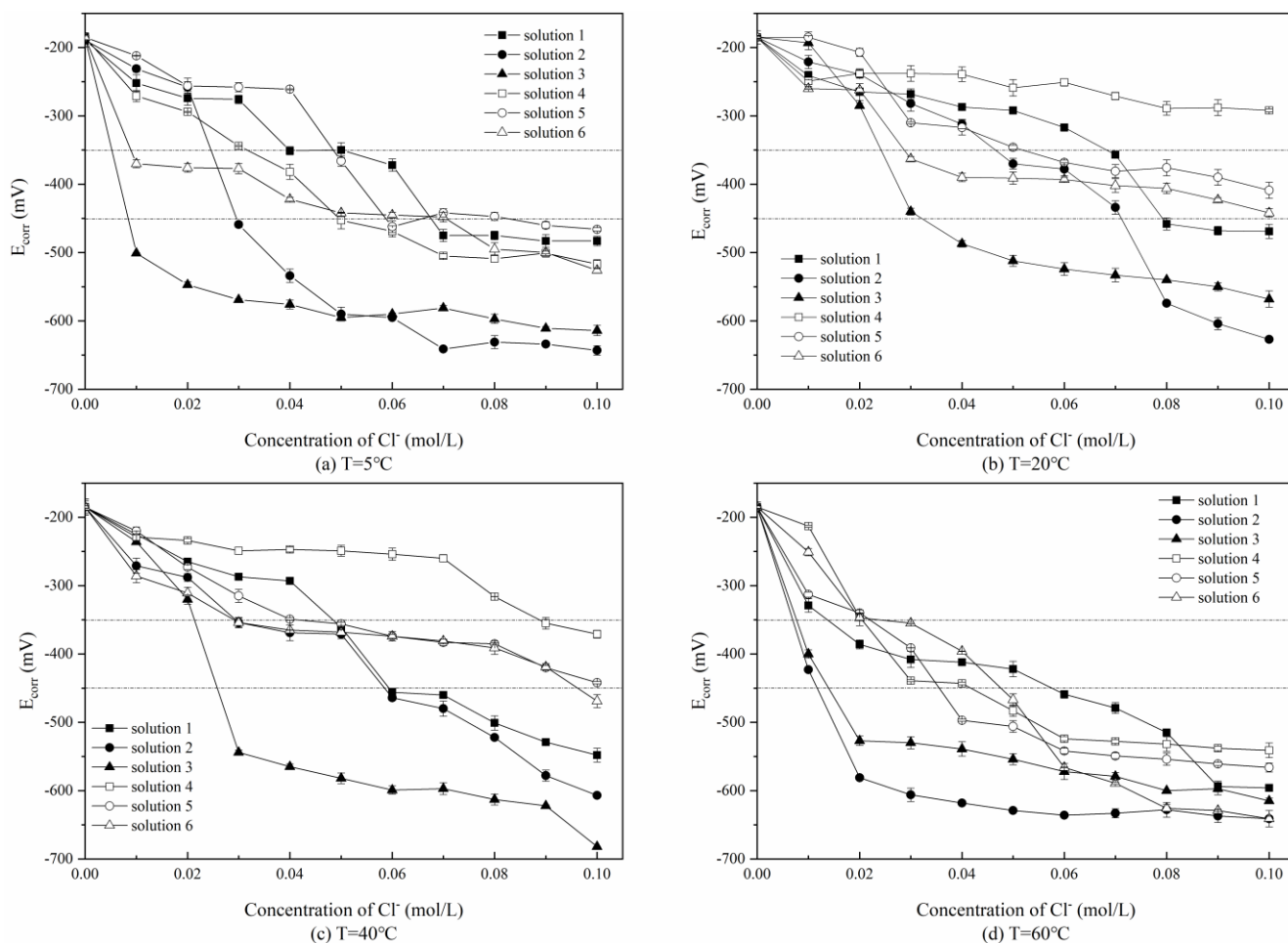


Figure 3. Variation in E_{corr} for the samples in Solutions 1-6 with the concentrations of Cl^- at four temperatures: (a) $T=5^\circ C$, (b) $T=20^\circ C$, (c) $T=40^\circ C$, (d) $T=60^\circ C$

It is suggested that corrosion begins when the E_{corr} values for samples range from -450 mV to -350 mV. The CTL in this paper was the chloride concentration when the E_{corr} values of samples descended to -350 mV. CTL values for samples in different solutions and at different temperatures are presented in Table 4. The impacts of temperature and carbonation on corrosion were reflected according to the CTL variations.

Table 4. The critical chloride level (CTL) for samples in solutions (1-6) at four temperatures

Solution	CTL (mol/L)			
	5°C	20°C	40°C	60°C
1	0.04	0.07	0.05	0.02
2	0.03	0.05	0.03	0.01
3	0.01	0.03	0.03	0.01
4	0.04	> 0.1	0.09	0.03
5	0.05	0.06	0.04	0.03
6	0.01	0.03	0.03	0.03

On the whole, the CTL values of the steel samples based on temperature were ordered from high to low as 60°C, 5°C, 40°C and 20°C. Compared to the standard curing temperature (20°C), both the lower temperature (5°C) and the higher temperatures (40°C & 60°C) increased the risk of chloride-induced corrosion of the samples. The increase was more significant at higher temperatures. In addition, the addition of NaHCO_3 also affected the corrosion behaviors of the samples. By comparing the CTL values in Solutions 1-3 and 4-6, the corrosion of steel samples in solutions without NaHCO_3 was generally more serious.

Moreover, samples in the three solutions showed different sensitivities to temperature changes and carbonations. The correlations between temperature and CTL values for samples are presented in Fig. 4., using the Spearman correlation test. The statistical significance was set at 5%. It was obvious that the samples in cement extracts were the most sensitive to temperature changes. For samples in cement-slag extracts, the correlations were the weakest. The correlation between solutions with or without NaHCO_3 followed the same trend. Synthetic Solution 1 and 2 were more appropriate for the simulation of steel corrosion under temperature changes and carbonation.

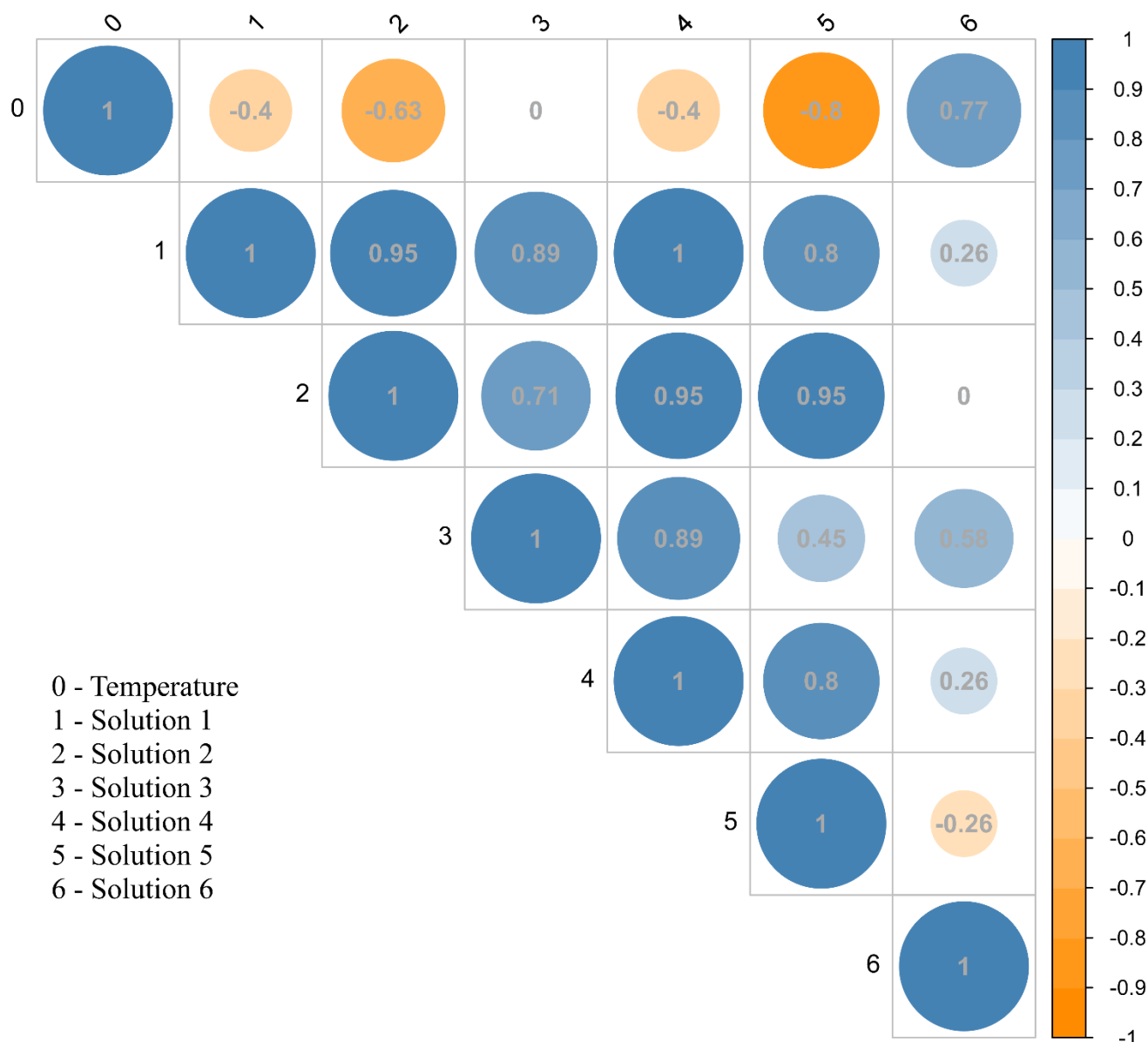


Figure 4. The correlation between temperature and CTL in six solutions

3.3. Linear polarization resistance

During the linear polarization resistance experiment, the curve of E-I was approximately a straight line, and the reinforced electrode polarization resistance (R_p) was represented as the slope of the line. According to the Stern-Geary theory [17], the corrosion current density (i_{corr}) for samples could be obtained by Eq.(1). Their i_{corr} values with the concentration of Cl^- are depicted in Fig. 5. Their corrosion conditions were structured in four levels based on the values and listed in Table 5.

$$i_{corr} = \frac{B}{R_p \cdot A} \tag{1}$$

where

B: the Stern-Geary constant, assumed to be 26 mV[18, 19],

A: the cross-sectional area of the steel electrode, 0.785 cm².

From Fig. 5., all the temperature, carbonation and types of synthetic solutions showed impacts on the corrosion of the samples.

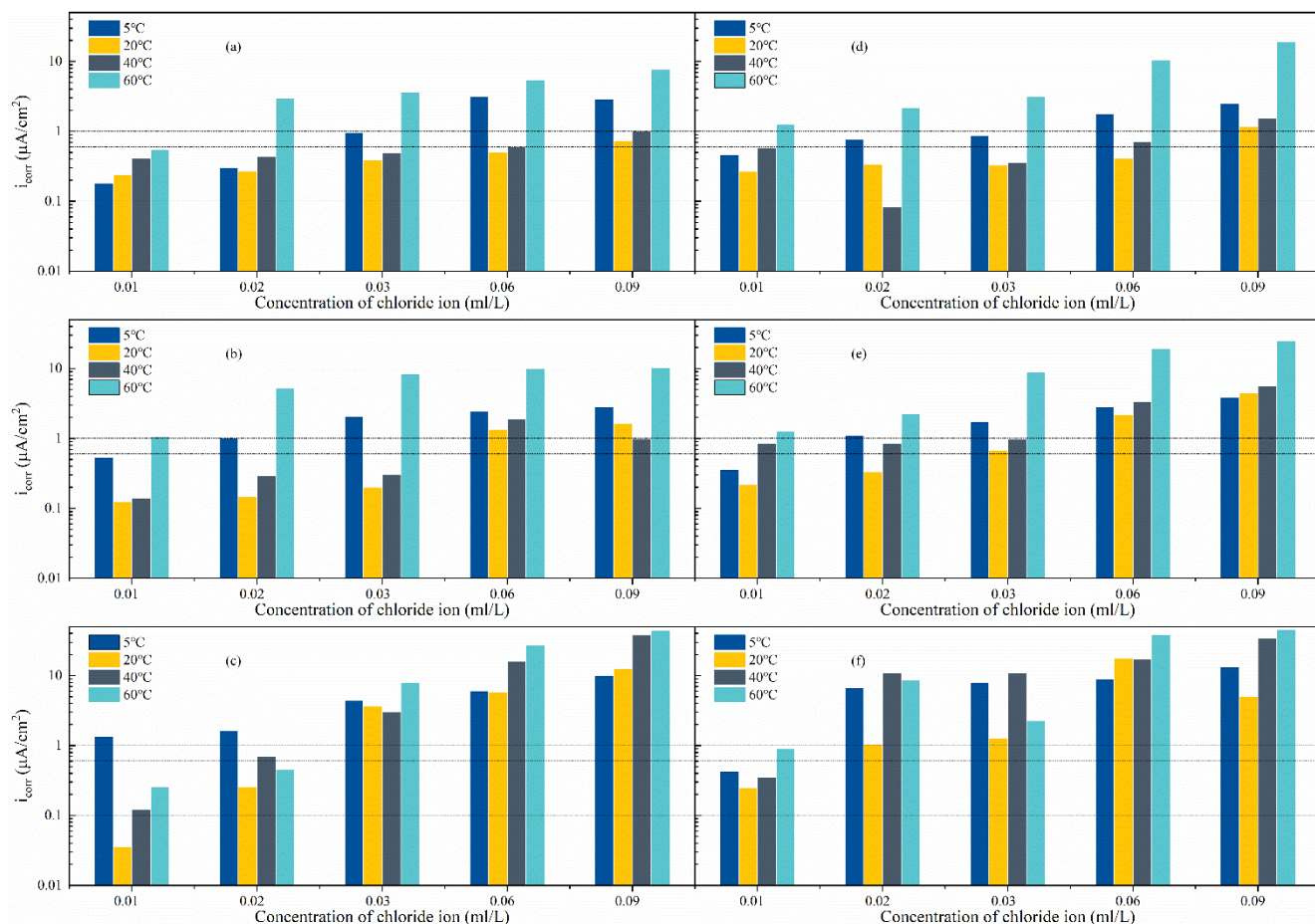


Figure 5. Variations in i_{corr} for the samples in solutions with different concentrations of Cl⁻ at four temperatures: (a-f) Solutions 1-6

Table 5. The corrosion conditions of samples based on the i_{corr} values [20]

i_{corr} ($\mu A/cm^2$)	Corrosion condition
<0.1	Passive condition
0.1~0.5	Low to moderate corrosion condition
0.5~1	Moderate to high corrosion condition
>1	High corrosion condition

3.3.1. Effect of temperature

Generally, samples were preferentially penetrated by chloride ions at higher temperatures. For samples in solutions without NaHCO₃, their i_{corr} values were initially enhanced at higher temperatures.

With the addition of chloride ions, i_{corr} values for samples exposed to 5°C and 60°C increased more rapidly than others. They appeared to be seriously corroded when the NaCl concentration reached 0.04 and 0.02 ml/L, but those exposed to 20°C were not corroded that badly. The i_{corr} values for samples exposed to 20°C and 40°C were similar until the NaCl concentration reached 0.09 ml/L. The values were over 1 $\mu\text{A}/\text{cm}^2$ at 0.1 mol/L NaCl.

The effect of temperature on the corrosion of steel samples was attributed to the three factors of the changes in pH values in the solutions, the kinetics of the corrosion reaction and the destruction of the passive film on the steel.

First, the pH values in solutions changed due to the variations in the solubility of $\text{Ca}(\text{OH})_2$ and the ionization product constant of water at four temperatures. When the temperature increased from 5°C to 60°C, the solubility of $\text{Ca}(\text{OH})_2$ decreased from 0.175 g to 0.12 g, and the ion product of water increased from 0.17×10^{-14} to 9.55×10^{-14} . The pH values in the solutions decreased when the temperature increased. The maximum difference among the pH values of solution 1 was monitored to be 1.5 among the four temperatures initially, agreeing with the calculation result. However, the decrease in pH values in solution was not equal to the corresponding drop in OH^- concentrations. Due to the dissolution mechanisms of strong electrolytes, the OH^- concentrations in solution 1 were assumed to be the same at the four temperatures. Hence, the changes in pH values in the solutions caused by temperature were not considered a main factor in this study.

Second, the corrosion of the steel in the solutions could be described using half-cell reactions [21], which were the anodic and cathodic reactions. The anodic reactions were related to the dissolution of Fe, which is shown in Eq. (2). The cathodic reaction was associated with the formation of hydroxide ions or hydrogen, playing a dominant role during the corrosion process. The possible reactions depended on the accessibility of oxygen and the pH values surrounding the steel surface [18]. In highly alkaline solutions, the reaction could be presented chemically as Eq. (3). Otherwise, the reaction like Eq. (4) also should be considered.



According to the Nernst equation, the cathodic electrode potential, relating to the cathodic reaction, can be presented as Eq. (5) [18, 22]. In Eq. (5), the cathodic electrode potential of the samples was connected to the temperature, the concentration of dissolved oxygen and the hydroxide ions in the solutions. The OH^- in the solutions mainly came from the dissolution of strong electrolytes. Taking solution 1 as an example, it could be assumed to be the same under different testing temperatures. However, the concentration of dissolved oxygen in the solutions changed with the temperature, and this effect could be quantified using Eq. (6) [7, 23].

$$E_c - E_c^0 = \frac{R_c T}{nF} \ln \frac{[\text{O}_2][\text{H}_2\text{O}]^2}{[\text{OH}^-]^4} \quad (5)$$

where

E_c^0 : the standard electrode potential of steel at the cathode, assumed to be 0.44 V,

R_c : the gas constant, 8.314 J/K,

F : the Faraday constant, 96,487 C,

T: the absolute temperature (K),

n: the number of electrons in the reaction equal to 4 or 2,

[O₂], [H₂O] and [OH⁻]: concentrations of O₂, H₂O and OH⁻ in solutions (mol/L), respectively.

$$\begin{aligned} \ln C_{O_2}^* = & -139.34411 + \left(\frac{1.575701 \times 10^5}{T} \right) - \left(\frac{6.642308 \times 10^7}{T^2} \right) \\ & + \left(\frac{1.243800 \times 10^{10}}{T^3} \right) - \left(\frac{8.621949 \times 10^{11}}{T^4} \right) - Chl[3.1929 \times 10^{-2} \\ & - \left(\frac{1.9428 \times 10^1}{T} \right) + \left(\frac{3.8673 \times 10^3}{T^2} \right)] \end{aligned} \quad (6)$$

where

C_{O₂}^{*}: the concentration of dissolved oxygen in water at 101.325 kPa, (mg/L),

T: the absolute temperature (K),

Chl: the concentration of chloride ions (mg/L).

When the temperature decreased from 60°C to 5°C, the maximum quantity of dissolved oxygen in the solutions increased from 4.72 mg/L to 12.74 mg/L. According to Eq. (5), the ratio of E_c-E_c⁰ for samples in solution 1 at the four temperatures was 0.8: 0.9: 1: 1.1 (from 60°C to 5°C). The cathodic electrode potential (E_c) for samples at 5°C was higher than that at 20°C, partially accounting for the severe corrosion of samples at 5°C. According to the cathodic electrode potential of steel, the changes in dissolved oxygen caused by temperature variations had greater impacts on corrosion than the temperature variation itself.

Third, the destruction of the passive film during the test procedures could not be ignored. The testing temperature of electrochemical measurement was set to 20°C. To achieve this temperature, samples were moved into the testing room in advance. During temperature variations, the degradation of passive films could not be avoided. According to Feng's investigations[24], the abrupt decline in temperature caused the depassivation of films. Greater changes in temperature led to worse degradation of the films. At the same time, the film was permeated by the added chloride ions. The interface between the passive films and the steel was attacked, accelerating the degradation of the films[25]. Referring to Fick's law, the diffusion progress was affected by temperature.

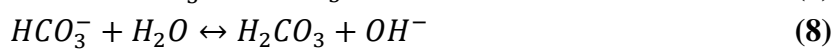
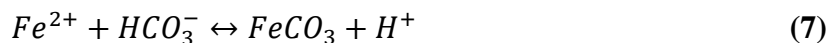
Considering the above factors, the effect of temperature could be understood. At 5°C, the diffusion and activity of chloride ions in the solutions were both limited. The degradation of passive films was initially slow. However, the electromotive forces of cells at 5°C were high due to the high level of dissolved oxygen concentrations. The film was also attacked by increasing chloride ions and temperature alternation. As a result, higher i_{corr} values were observed at low temperatures.

From 20°C to 60°C, the concentration of dissolved oxygen in solutions decreased, but the activity of chloride ions, electromotive force and degradation of passive films all increased. With increasing temperature, the impacts of the dissolved oxygen quantity on the corrosion of the samples were gradually reduced. The acceleration of reaction rates became more significant. This accounted for the similar corrosion of samples at 20°C and 40°C, along with the severe corrosion at 60°C.

3.3.2. Effect of carbonation

In Fig. 5.(d), the corrosion of the samples was suppressed at 5, 20 and 40°C but accelerated at 60°C in solutions with NaHCO₃. According to the buffering influence of HCO₃⁻ [26], as seen in Eq. (7), higher concentrations of HCO₃⁻ promoted the formation of FeCO₃, but lower concentrations had the opposite effect. FeCO₃ was able to attach to the surface of passive layers, helping to resist chloride ions. Moreover, at the beginning of the test, the concentration of bicarbonate ions in solutions was much larger than that of chloride ions. The difference in concentrations caused the bicarbonate ions to be more easily absorbed into the barrier layer oxygen vacancy sites. The suppression effect of the bicarbonate ions was demonstrated during the test [14, 27].

However, FeCO₃ could not exist stably if the pH value of the solution was over 9.5, as shown in Eq. (7) [28]. The hydrolysis equilibrium of HCO₃⁻ in solutions can be described by Eq. (8), and it is affected by temperature. When temperatures increased, the equilibrium of Eq. (8) shifted to the right side. Then, the pH value of the solutions increased, and the concentration of HCO₃⁻ decreased. In addition, the HCO₃⁻ in the solutions would start to decompose if the temperature was over 50°C. At 60°C, the concentration of HCO₃⁻ in the solutions decreased to a low level. Meanwhile, the concentration of OH⁻ in the solutions was high enough to make FeCO₃ unstable. Then, the equilibrium of Eq. (7) shifted to the left side. Without promoting the formation of FeCO₃, the existence of HCO₃⁻ only decreased the pH value of solutions at 60°C, destroying the passive film on the steel surface.



3.3.3. Effect of simulated concrete pore solution

Apart from the temperature and carbonation, the types of synthetic solutions also had impacts on the steel corrosion. For those specimens in the three solutions without NaHCO₃, their *i*_{corr} values exhibited different tendencies with temperature. In cement extracts (solution 2), the development of *i*_{corr} values for samples showed some differences. When exposed at 5°C and 60°C, *i*_{corr} values for these samples were very high initially, but increased slowly in the following test. At 20°C and 40°C, *i*_{corr} values for samples were low at the beginning, but increased obviously at certain NaCl levels, and then tended to be similar. In cement-slag extracts (solution 3), the development appeared generally like those in solution 2, but the *i*_{corr} values of the samples were initially lower and increased more quickly.

Different sensitivities of samples in three solutions to the temperature could be anticipated due to the different compositions among these solutions. Firstly, their pH values were slightly different. Other than solution 1, the concentrations of Ca(OH)₂ in the cement extract or cement-slag extract were unsaturated, reducing the pH value. As shown in Table 3., the lower pH corresponded to more severe corrosion in solutions 2 and 3.

Second, the hydration products in the two extract solutions accounted for the differences. Solution 1 was the mixture of Ca(OH)₂, KOH and NaOH. There was no cementitious material in it. Solutions 2 and 3 were the cement extract and slag-cement extract, respectively. Due to the hydration reactions during the preparation, the chloride ions could be physically absorbed or chemically bonded

to the hydration products in these two solutions, controlling the corrosion of the samples. In addition, some flocculent precipitates on the surface of steel samples in extracts were monitored during the test. These could resist the diffusion of oxygen and chloride ions [29]. Nevertheless, the bonding capacity of hydration products was very limited. The inhibition effect did not work out with the continuous addition of Cl^- in solutions. Finally, samples in solutions 2 and 3 were corroded slightly at the initial stage but seriously with continuous addition of Cl^- .

The severe corrosion at 5°C initially, it could be explained by the chemical equilibrium shift of Eq. (3). Due to the increase in the degree of dissolved oxygen and the drop in OH^- concentrations in the extracts, the equilibrium of the cathodic reaction was shifted toward the right side. In addition, the type and amount of hydration products in these two solutions were different. In cement systems, more Afm salts were produced [30], but more hydrated calcium aluminates were formed in cement-slag systems [31]. The better ability of hydrated calcium aluminates to bond to Cl^- led to only slight corrosion of the samples at 60°C with 0.01 and 0.02 mol/L NaCl.

In addition, unlike samples in solution 4, the corrosion of samples in solutions 5 and 6 generally appeared to be worse than those in solution without NaHCO_3 . This was attributed to the reactions between HCO_3^- and hydration products [32]. The concentration of HCO_3^- dropped to a low level due to these reactions, and the equilibrium of Eq. (7) tended to shift to the left side.

3.4. Electrochemical impedance spectroscopy

Taking samples in solutions 2 and 5 as examples, their Nyquist plots of EIS at four temperatures are shown in Fig. 6. The Bode plots of the samples in solution 2 are shown in Fig. 7. In Fig. 6., the curves of all samples were parts of capacitive loops. With the addition of chloride ions, the diameters of the capacitive loops decreased. This was mainly due to the destruction of the passive film on the steel surface during corrosion. In Fig. 7., similar results could be found. The low-frequency impedance modulus decreased considerably with the addition of 0.08 mol/L Cl^- in Fig. 7. (a) & (c), which indicated that corrosion actively occurred on the steel surface.

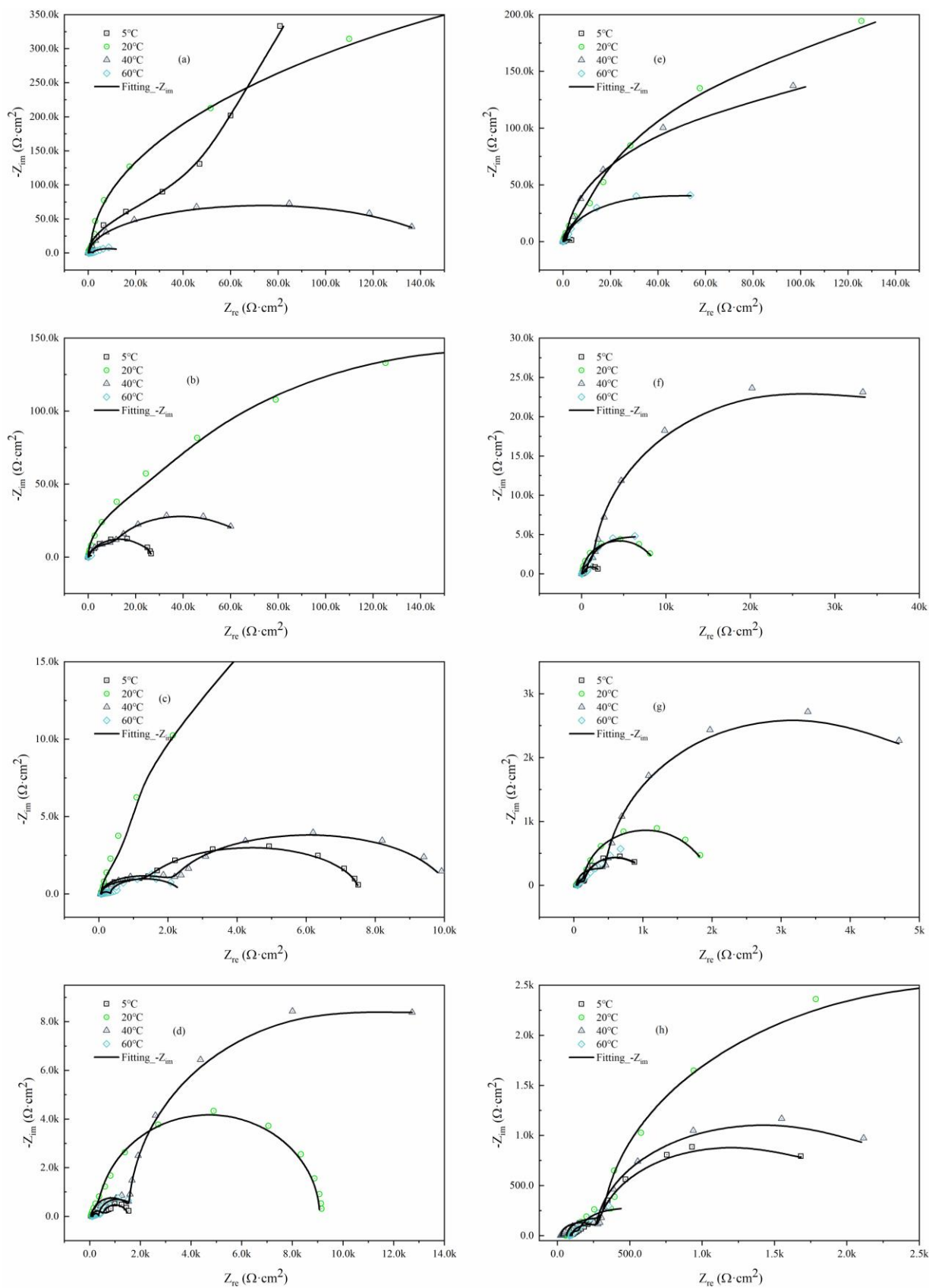


Figure 6. Nyquist plots for the samples in Solutions 2 and 5 with Cl⁻ at four temperatures: (a-d) Solution 2 with 0.01, 0.03, 0.06 and 0.09 mol/L Cl⁻, (e-h) Solution 5

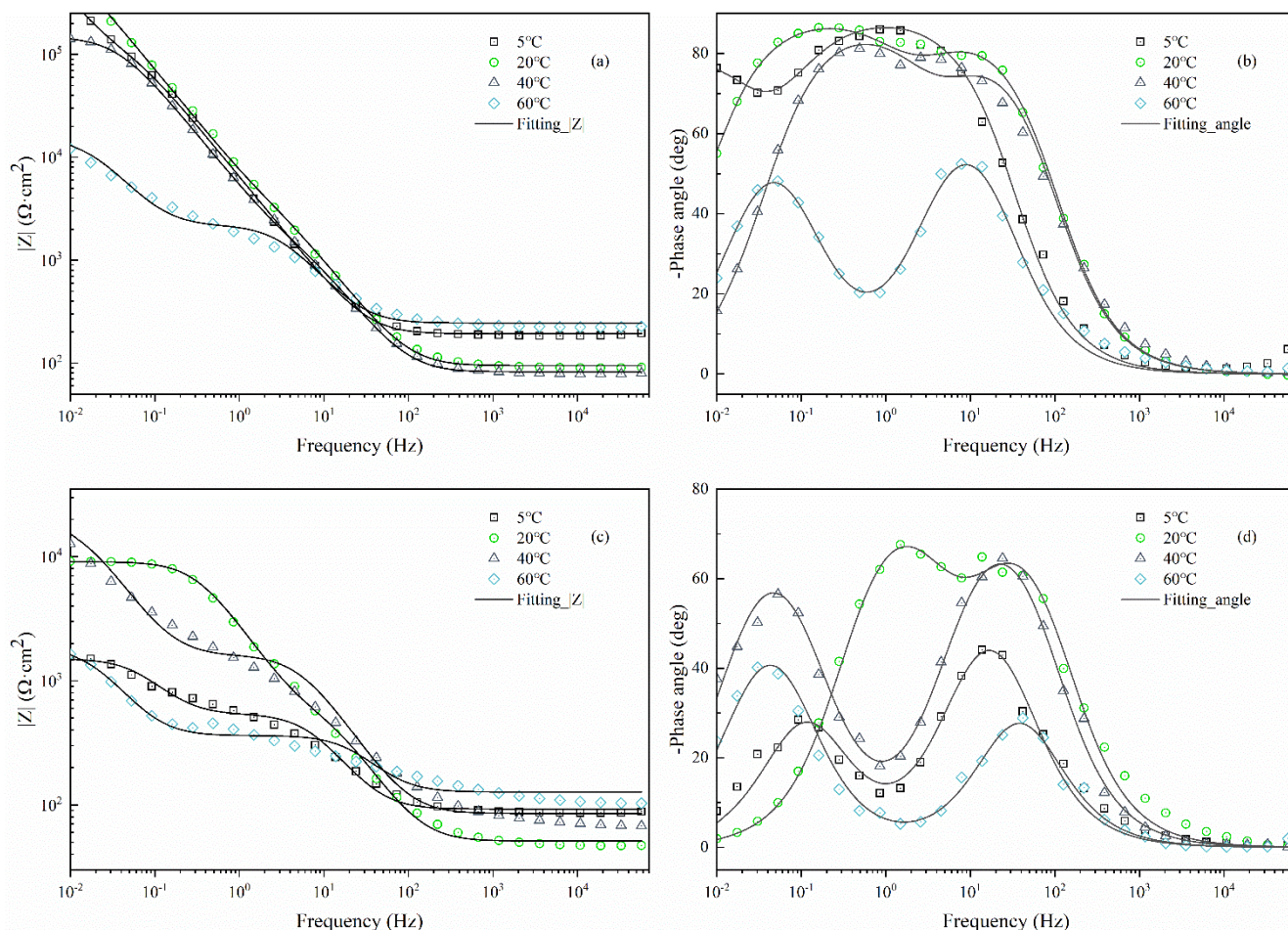


Figure 7. Bode plots for the samples in Solution 2 with Cl⁻ at four temperatures: (a & c) impedance modulus plots with 0.01 and 0.09 mol/L Cl⁻, (b & d) phase angle plots with 0.01 and 0.09 mol/L Cl⁻

It is widely accepted that the EIS curve at high frequency closely corresponds to the resistance between the corrosion solution and the working electrode. In the curves, this resistance was related to the diameters of the capacitive reactance arc. To analyze the deterioration of passive films during corrosion, an equivalent-circuit model was applied and demonstrated in Fig. 8. [33, 34]. R_s is the solution resistance. R_f is the passivation and adsorption film resistance, and C_f is the capacitance related to those resistances. R_{ct} and C_{dl} are the charge transfer resistance and the electric double-layer capacitance, respectively. They were related to the conditions of the corrosion reaction on the steel surface [35, 36]. The fitting results of the R_f and R_{ct} values calculated from the models are listed in Table 6.

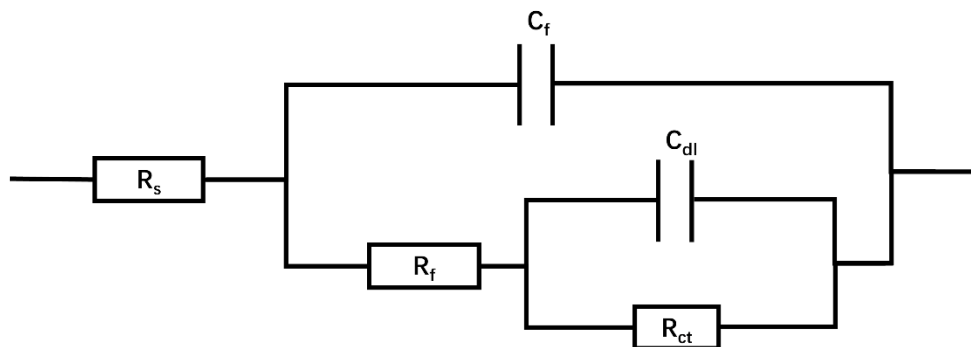


Figure 8. Equivalent-circuit model of the measured EIS results.

Table 6. The passivation film resistance (R_f) and corrosion reaction resistance (R_{ct}) of steel ($10^3 \Omega \cdot \text{cm}^2$)

Concentration of Cl^- (mol/L)	Solution 2				Solution 5				
	0.01	0.03	0.06	0.09	0.01	0.03	0.06	0.09	
R_f	5°C	219.3	4.581	1.878	0.4852	0.7743	0.1648	0.1238	0.1399
	20°C	13.31	12.04	8.979	0.8926	53.95	0.1636	0.1641	0.3245
	40°C	4.179	17.00	2.389	1.384	9.184	2.848	0.5101	0.2657
	60°C	2.013	0.2022	0.3175	0.2768	3.179	0.626	0.0745	0.0833
R_{ct}	5°C	3494	21.89	5.620	1.015	4.225	1.442	0.8787	0.8412
	20°C	1041	186.9	95.57	8.135	381.2	8.695	1.737	5.176
	40°C	142.4	51.39	7.612	16.95	277.3	46.34	5.310	2.288
	60°C	12.77	2.012	2.016	1.498	81.83	9.523	0.9461	0.5126

In Table 6., the R_f and R_{ct} values of the samples were generally in accord with the evolution of E_{corr} and i_{corr} . With 0.01 mol/L chloride ion, the R_f and R_{ct} values of the specimens in solution 2 generally decreased with increasing temperature. This coincided with the explanation that the degradation of passive films and rates of chemical reactions were both promoted at higher temperatures. When chloride ions were added, the values declined quickly. This showed the degradation of films and promotion of electrochemical reactions. The development of these two values at 5°C were worth noting. They were lower than those of specimens at 20°C and 40°C when the chloride ion concentration was at 0.03 mol/L. The decline represented the greater damage of passive films and faster corrosion reactions at the lower temperature. Due to the low temperature, the film was still passivated in the initial experiment. However, with increasing chloride ions and temperature alternation, the film degraded more quickly. Meanwhile, with the higher concentration of dissolved oxygen at 5°C, the corrosion reaction was also faster. In

addition, with the existence of NaHCO_3 in solution 5, the R_f and R_{ct} values of the samples all decreased at the four temperatures.

4. CONCLUSIONS

In summary, the effects of temperature, carbonation, and the types of synthetic solution on the chloride corrosion of steel reinforcement have been studied in this paper. A relatively wide range of temperatures (from 5°C to 60°C), the high concentration of bicarbonate ions (0.2 mol/L) and three kinds of synthetic pore solutions were applied in this study. The principal conclusions are as follows:

(1) The temperature did have an impact on the corrosion process of the steel samples. Over 20°C , the corrosion of steel was more serious at higher temperatures. This was mainly due to the acceleration of the corrosion reaction and the dissolution of passive films. The lower temperature (5°C) also promoted corrosion, which was accounted for by the higher concentration of dissolved oxygen in the solutions.

(2) With the addition of 0.2 mol/L NaHCO_3 , the corrosion of samples in the solutions appeared to be inhibited under 40°C but accelerated at 60°C . The buffering influence of the bicarbonate ions accounted for the difference. In addition, using NaHCO_3 to simulate the effect of carbonation was not appropriate at temperatures over 50°C considering decomposition.

(3) Samples in three synthetic solutions showed different sensitivities to temperature and carbonation. The traditional synthetic solution (solution 1) and cement extracts (solution 2) were more appropriate in the test.

ACKNOWLEDGEMENTS

The authors would like to acknowledge the support provided by the Fundamental Research Funds for the Central Universities (No. 2018B691X14), the Postgraduate Research & Practice Innovation Program of Jiangsu Province (KYCX18_0571), and the National Natural Science Foundation of China (No. 52078183).

References

1. R. Liu, L. H. Jiang, G. H. Huang, Y. R. Zhu, X. R. Liu, H. Q. Chu and C. S. Xiong, *Constr. Build. Mater.*, 113 (2016) 90-95.
2. P. Xu, L. H. Jiang, M. Z. Guo, J. Zha, L. Chen, C. Chen and N. Xu, *Constr. Build. Mater.*, 223 (2019) 352-359.
3. R. Liu, L. H. Jiang, J. X. Xu, C. S. Xiong and Z. J. Song, *Constr. Build. Mater.*, 56 (2014) 16-20.
4. K. A. A. Al-Sodani, O. S. B. Al-Amoudi, M. Maslehuddin and M. Shameem, *Constr. Build. Mater.*, 163 (2018) 97-112.
5. A. A. Adewumi, M. Maslehuddin, S. U. Al-Dulaijan and M. Shameem, *Eur. J. Environ. Civ. En.*, 25 (2018) 452-467.
6. J. Z. Hu, X. Q. Cheng, X. G. Li, P. C. Deng and G. Wang, *J. Chem-NY.*, 2015 (2015) 1 -6.
7. M. Pour-Ghaz, O. B. Isgor and P. Ghods, *Corros. Sci.*, 51 (2009) 415-425.
8. Y. Lu, H. Jing, Y. Han and L. Xu, *Mater. Chem. Phys.*, 178 (2016) 160-172.

9. Y. Shen, Y. Dong, H. Li, X. Chang, D. Wang, Q. Li and Y. Yin, *Int. J. Electrochem. Sci.*, 13 (2018) 6310-6326.
10. M. Jeannin, D. Calonnec, R. Sabot and P. Refait, *Electrochim. Acta*, 2011 (2011) 1466-1475.
11. G. S. Duffó and S. B. Farina, *Cem. Concr. Res.*, 88 (2016) 211-216.
12. J. J. Shi, J. Ming and W. Sun, *Corros. Sci.*, 133 (2018) 288-299.
13. A. Moragues, A. Macias and C. Andrade, *Cem. Concr. Res.*, 17 (1987) 173-182.
14. Y. T. Tan, S. L. Wijesinghe and D. J. Blackwood, *Corros. Sci.*, 88 (2014) 152-160.
15. L. H. Jiang, G. H. Huang, J. X. Xu, Y. R. Zhu and L. L. Mo, *Constr. Build. Mater.*, 30 (2012) 516-521.
16. B. Isgor, U. Angst, M. Geiker, C. Halmen, C. Hansson, J. Pacheco, D. Tepke, D. Trejo and P. Vaddey, *RILEM. Tech. Lett.*, 4 (2019) 22 -32.
17. M. Stern and A. L. Geary, *J. Electrochem. Soc.*, 104 (1957) 56-63.
18. S. Ahmad, *Cem. Concr. Compos.*, 25 (2003) 459-471.
19. C. Andrade and J. A. González, *Mater. Corros.*, 29 (1978) 515-519.
20. L. Freire, M. A. Catarino, M. I. Godinho, M. J. Ferreira, M. G. S. Ferreira, A. M. P. Simoes and M. F. Montemor, *Cem. Concr. Compos.*, 34 (2012) 1075-1081.
21. C. M. Hansson, *Cem. Concr. Res.*, 1984 (1984) 574-584.
22. Z. P. Bazant, *Journal of the Structural Division*, ASCE, 1979 (1979) 1137-1153.
23. L. S. Clescerl, A. E. Greenberg and A. D. Eaton, *Standard Methods for the Examination of Water and Wastewater*, American Public Health Association, (1999) Washinton, DC, USA.
24. X. Feng, T. Wu, J.-l. Luo and X. Lu, *Cem. Concr. Compos.*, 112 (2020) 103651.
25. B. Zhang, J. Wang, B. Wu, X. W. Guo, Y. J. Wang, D. Chen, Y. C. Zhang, K. Du, X. L. Ma, E. E. Oguzie and X. L. Ma, *Nat. Commun.*, 2018 (2018)
26. M. Moreno, W. Morris, M. G. Alvarez and G. S. Duffo, *Corros. Sci.*, 46 (2004) 2681-2699.
27. D. Macdonald and X. Lei, 2, *J. Electrochem. Soc.*, 163 (2016) C738-C744.
28. M. B. Valcarce, C. Lopez and M. Vazquez, *J. Electrochem. Soc.*, 159 (2012) C244-C251.
29. J. Shi, J. Ming and W. Sun, *Constr. Build. Mater.*, 155 (2017) 992-1002.
30. S. Rahimi-Aghdam, Z. P. Bazant and M. J. A. Qomi, *J. Mech. Phys. Solids.*, 99 (2017) 211-224.
31. M. Otieno, H. Beushausen and M. Alexander, *Cem. Concr. Compos.*, 46 (2014) 56-64.
32. D. J. Anstice, C. L. Page and M. M. Page, *Cem. Concr. Res.*, 35 (2005) 377-383.
33. S. B. Jiang, L. H. Jiang, Z. Y. Wang, M. Jin, S. Y. Bai, S. Q. Song and X. C. Yan, *Constr. Build. Mater.*, 150 (2017) 238-247.
34. A. Bautista, E. C. Paredes, S. M. Alvarez and F. Velasco, *Corros. Sci.*, 102 (2016) 363-372.
35. M. Wu and J. Shi, *Corros. Sci.*, 183 (2021) 109326.
36. P. Xu, J. Zhou, G. Li, P. Wang, P. Wang, F. Li, B. Zhang and H. Chi, *Constr. Build. Mater.*, 288 (2021) 123101